Supplementary Materials

for

A Novel Framework for Molecular Characterization of Atmospheric Organic Aerosol Based on Collision Cross Section and Mass-to-Charge Ratio

X. Zhang[1], J. E. Krechmer[2,3], M. Groessl[4], W. Xu[1], S. Graf[4], M. Cubison[4],

J. T. Jayne[1], J.L. Jimenez[2,3], D. R. Worsnop[1], and M. R. Canagaratna[1]

[1] Center for Aerosol and Cloud Chemistry, Aerodyne Research Inc., Billerica, MA 01821, USA

[2] Department of Chemistry and Biochemistry, University of Colorado, Boulder, CO 80309, USA

[3] Cooperative Institute for Research in Environmental Sciences, Boulder, CO 80309, USA

[4] TOFWERK, CH-3600 Thun, Switzerland

Correspondence to: M. R. Canagaratna (mrcana@aerodyne.com)

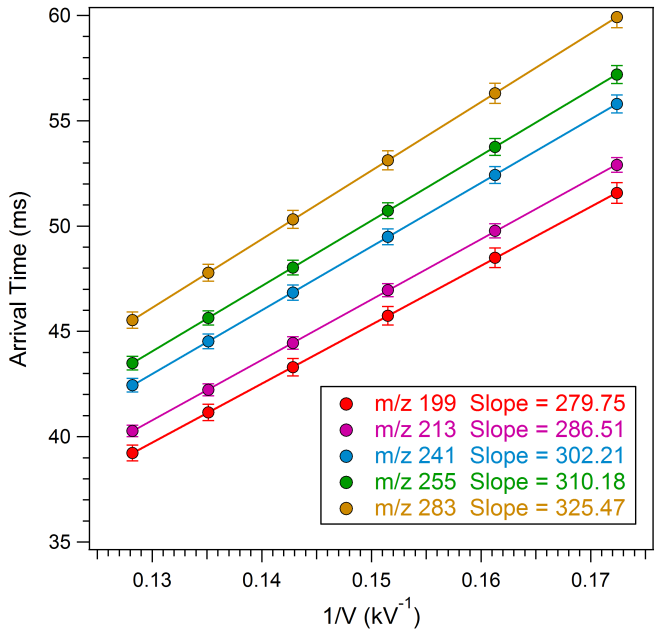

Figure S1. Linear regression of the recorded arrival time (t_a) for the deprotonated C_{12} (*m/z* 199), C_{13} (*m/z* 213), C_{15} (*m/z* 241), C_{16} (*m/z* 255), and C_{18} (*m/z* 283) *mono*-carboxylic acids on the inverse of the drift voltage in ~ 1019 *mbar* of nitrogen gas at 340 K. Three replicate mobility measurements were performed and the deviations in the calculated mobility constants are within ±0.95%, ±0.67%, ±0.77%, ±0.74% and ±0.84%, respectively.

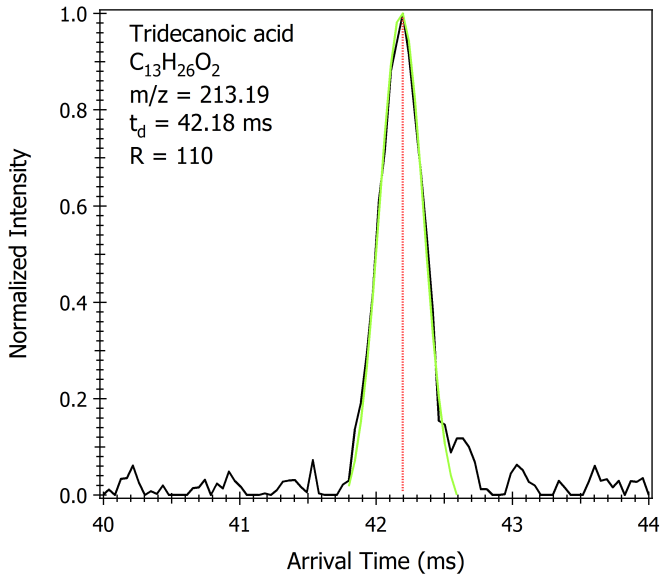

Figure S2. Arrival time distribution for the deprotonated tridecanoic acid (*m/z* = 213.19) with a drift voltage of 7.42 kV in ~ 1019 *mbar* of nitrogen gas at 340 K.

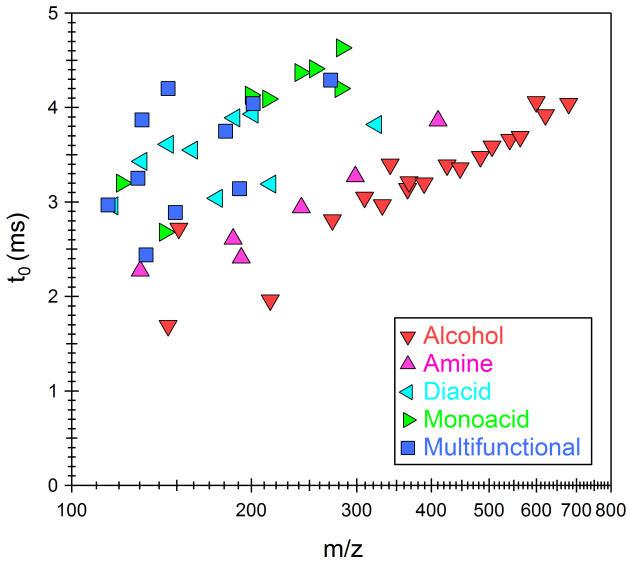

Figure S3. Time of the ion spent from the exit of the drift tube to the MS detector (t_0) as a function of mass-to-charge ratio (*m/z*). For a selected organic class, t_0 is proportional to $\sqrt{m/z}$ due to the time-of-flight separation. For different organic classes, t_0 values span a large range under the same *m/z* value due to different CID voltages applied (0 – 6 V) at the quadruple interface during the measurement.

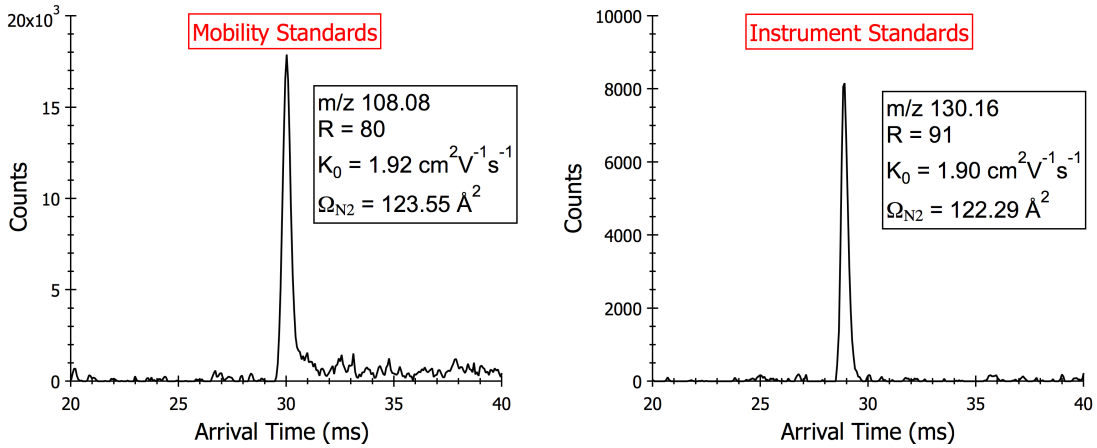

Figure S4. Arrival time distributions for the mobility standard 2,4-lutidine (*m/z* = 108.08) and the instrument standard tetraethyl ammonium iodide (*m/z* = 130.16) with a drift voltage of 7.42 kV in ~ 1019 *mbar* of nitrogen gas at 340 K. Also shown are their calculated reduced mobility constants (K_0) and collision cross sections (Ω_{N_2}).

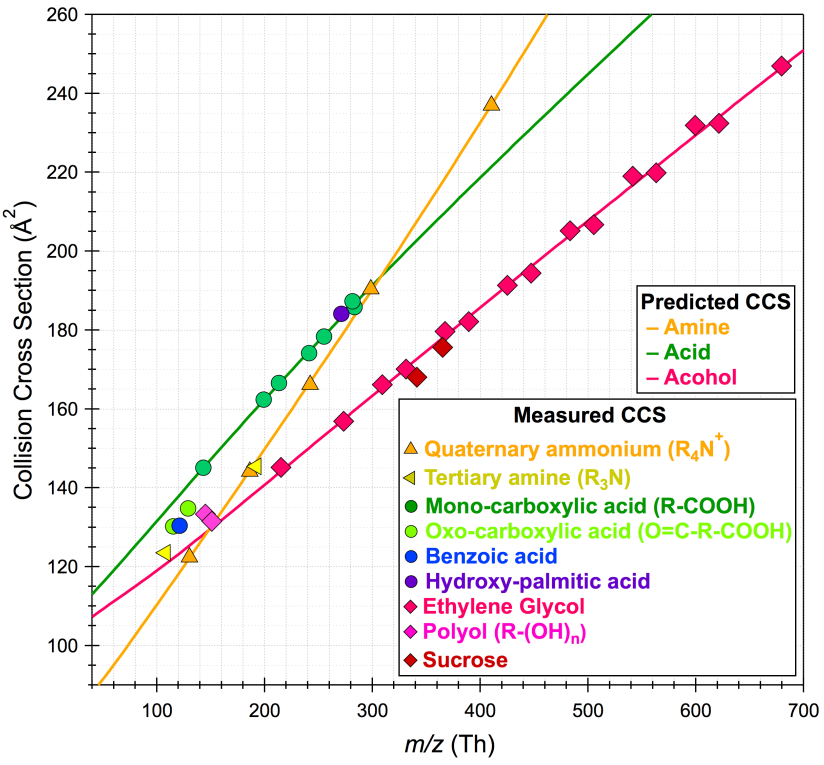

Figure S5. A unified version of Figure 3 in the main text showing the separation of amines, alcohols, and carboxylic acids.

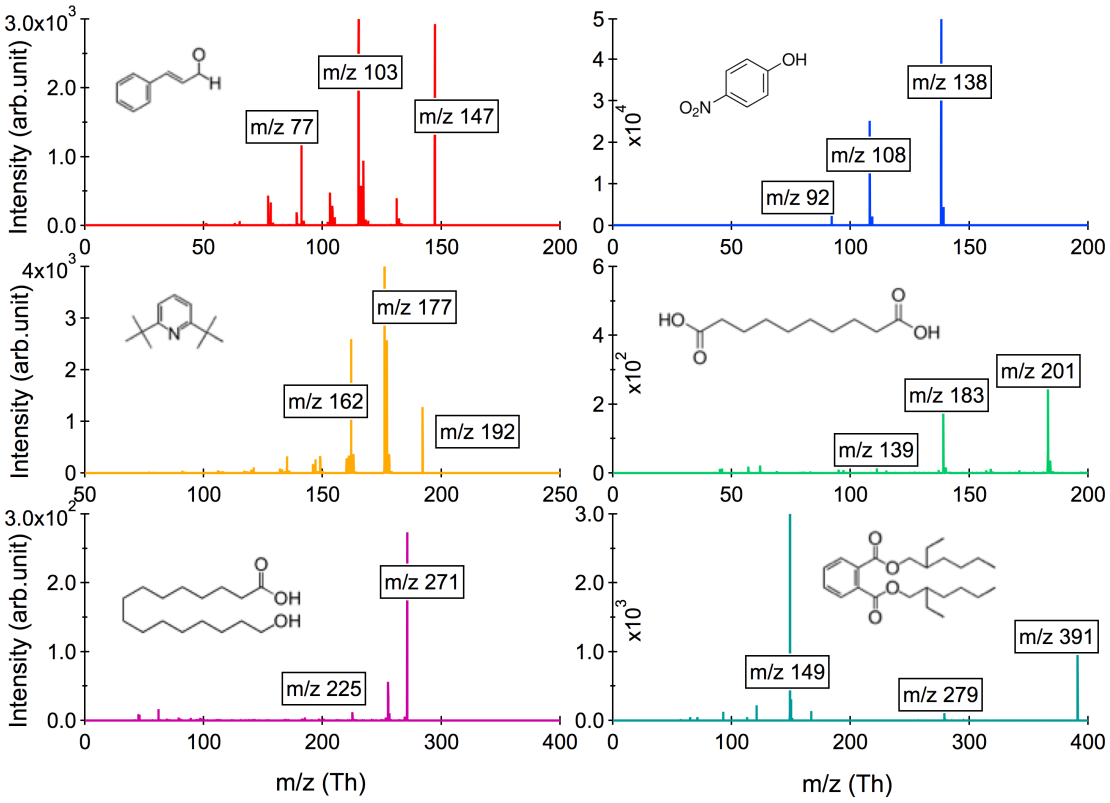

Figure S6. Mobility selected MS spectra for the precursor and corresponding CID-induced fragment ions for cinnamaldehyde, dioctyl phthalate, 2,6-di-tert-butylpyridine, 4-nitrophenol, 16-hydroxyhexadecanoic acid, and sebacic acid.

Table S1. Comparison of collision cross section values (Ω_{N_2}) for small ionic compounds measured from this study with those reported in literatures.

Name	*m/z*	Ω_{N_2}		% Diff.
		This study	Literatures	
Tetraethylammonium	130	122.09	122.2[(a)]	-0.09
Tetrapropylammonium	186	143.75	143.8[(a)]	-0.03
Tetrabutylammonium	242	165.77	166.0[(a)]	-0.14
Tetrapentylammonium	298	189.96	190.1[(a)]	-0.00
Tetraheptylammonium	410	236.46	236.8[(a)]	-0.14
Malic acid	133	111.41	113.9[(b)]	-2.24
Citric acid	191	123.02	125.5[(b)]	-1.80

Data source: [(a)] Campuzano et al. (2012) and [(b)] Forsythe et al. (2015).

Table S2. Predicted collision cross sections ($\Omega_{N_2\_mod}$) by the (12-4) core model with best-fit parameters.

	m/z	r_m (Å)	*a* (Å)	ε (J)	$\Omega_{N_2\_mod}$ (Å^2)	$\Omega_{N_2\_exp}$ (Å^2)	% Diff.
Amine	130.16	7.35	2.20	1.91e-21	122.0	122.3	-0.22
	186.10	8.24	2.47	1.21e-21	144.2	144.0	0.14
	242.17	9.06	2.72	8.25e-22	166.6	166.0	0.37
	298.35	9.84	2.95	5.92e-22	189.5	190.2	-0.38
	410.47	11.34	3.40	3.36e-22	236.9	236.7	0.06
Carboxylic acid	143.11	7.55	3.02	3.16e-21	144.9	144.9	0.00
	199.17	8.20	3.28	2.28e-21	162.0	162.2	-0.11
	213.19	8.34	3.34	2.13e-21	166.2	166.4	-0.11
	241.22	8.62	3.45	1.87e-21	174.4	174.0	0.25
	255.23	8.75	3.50	1.76e-21	178.5	178.1	0.18
	283.26	9.01	3.60	1.56e-21	186.5	185.6	0.44
	281.25	8.99	3.60	1.58e-21	185.9	187.1	-0.66
Alcohol	273.17	8.02	3.21	2.49e-21	157.2	156.7	0.30
	309.23	8.31	3.32	2.16e-21	165.3	166.0	-0.43
	331.21	8.48	3.39	1.99e-21	170.2	169.9	0.17
	367.27	8.74	3.50	1.76e-21	178.3	179.5	-0.67
	389.24	8.90	3.56	1.64e-21	183.1	182.0	0.65
	425.31	9.15	3.66	1.47e-21	191.1	191.1	0.00
	447.28	9.30	3.72	1.38e-21	196.0	194.3	0.86
	483.35	9.54	3.82	1.24e-21	203.9	205.0	-0.56
	505.32	9.68	3.87	1.17e-21	208.6	206.5	1.03
	541.39	9.91	3.96	1.07e-21	216.5	218.8	-1.07
	563.36	10.05	4.02	1.01e-21	221.3	219.6	0.74
	599.42	10.27	4.11	9.27e-22	229.1	231.6	-1.11
	621.40	10.40	4.16	8.80e-22	233.8	232.2	0.71
	679.44	10.74	4.30	7.73e-22	246.3	246.7	-0.14

References:

Campuzano, I., Bush, M. F., Robinson, C. V., Beaumont, C., Richardson, K., Kim, H., and Kim, H. I.: Structural characterization of drug-like compounds by ion mobility mass spectrometry: comparison of theoretical and experimentally derived nitrogen collision cross sections, Anal. Chem., 84, 1026-1033, 2012.

Forsythe, J. G., Petrov, A. S., Walker, C. A., Allen, S. J., Pellissier, J. S., Bush, M. F., Hud, N. V., and Fernandez, F. M.: Collision cross section calibrants for negative ion mode traveling wave ion mobility-mass spectrometry, Analyst, 140, 6853-6861, 2015.